DMD Fast Forward. Published on August 25, 2008 as doi:10.1124/dmd.108.023150

DMD #23150

Intravenous Formulation of HET0016 for Inhibition of Rat Brain 20-Hydroxyeicosatetraenoic Acid (20-HETE) Formation

Ying Mu, Megan M. Klamerus, Tricia M. Miller, Lisa C. Rohan, Steven H. Graham, and Samuel M. Poloyac.

University of Pittsburgh School of Pharmacy, Department of Pharmaceutical Sciences, Pittsburgh, PA 15261 (SMP, TM, MK, YM, LCR); Magee's Women's Research Institute, Pittsburgh, PA 15213 (LCR); University of Pittsburgh School of Medicine, Department of Neurology, Pittsburgh, PA 15261 (SHG); Geriatric Research Educational and Clinical Center, V.A. Pittsburgh Healthcare System (SHG).

Running Title: Intravenous HET0016 for Selective Brain 20-HETE Inhibition

Corresponding Author: Samuel M. Poloyac, Pharm.D., Ph.D.

Assistant Professor

807 Salk Hall

School of Pharmacy

University of Pittsburgh

Pittsburgh, PA 15261

Phone: 412-624-4595

Fax: 412-383-7436

E-mail: poloyac@pitt.edu

Number of Text Pages: 19

Number of Tables: 2

Number of Figures: 7

Number of References: 22

Word Count:

Abstract: 234

Introduction: 606

Discussion: 907

Non-standard Abbreviations: hydroxyeicosatetraenoic acid (HETE); epoxyeicosatrienoic acid (EET); cytochrome P450 (CYP); 17-octadecynoic acid (17-ODYA), N-methylsulfonyl-12,12-dibromododec-11-enamide (DDMS), N-Hydroxy-N'-(4-n-butyl-2-methylphenyl)formamidine (HET0016), N-(3-chloro-4-morphlin-4yl-N'hydroxyimidoformamide (TS-011), hydroxypropyl-beta-cyclodextrin (HPβCD).

ABSTRACT

N-Hydroxy-N'-(4-n-butyl-2-methylphenyl)formamidine (HET0016) is a potent inhibitor of 20-hydroxyeicosatetraenoic acid (20-HETE) formation by specific cytochrome P450 (CYP) isoforms. Previous studies have demonstrated that administration of HET0016 inhibits brain formation of 20-HETE and reduces brain damage in a rat model of thromboembolic stroke. Delineation of the dose, concentration, neuroprotective effect relationship of HET0016 has been hampered by the relative insolubility of HET0016 in aqueous solutions and the lack of information concerning the mechanism and duration of HET0016 inhibition of brain 20-HETE formation. Therefore, it was the purpose of this study to develop a water soluble formulation of HET0016 suitable for intravenous (iv) administration and to determine the time course and mechanism of brain 20-HETE inhibition after *in vivo* dosing. In this study we report that HET0016 is a non-competitive inhibitor of rat brain 20-HETE formation, which demonstrates a tissue concentration range for brain inhibition. In addition, we demonstrate that complexation of HET0016 with hydroxypropyl-β-cyclodextrin (HPβCD) results in increased aqueous solubility of HET0016 from 34.2 ± 31.2 μg/mL to 452.7 ± 63.3 μg/mL. Administration of the complex containing formulation as a single HET0016 iv dose (1 mg/kg) rapidly reduced rat brain 20-HETE concentrations from 289 pmol/g to 91pmol/g. Collectively, these data demonstrate that the iv formulation of HET0016 rapidly penetrates the rat brain and significantly inhibits 20-HETE tissue concentrations. These results will enable future studies to determine biopharmaceutics of HET0016 for inhibition of 20-HETE after cerebral ischemia.

Cytochrome P450 (CYP) isoforms constitute a superfamily of enzymes that typically catalyze the incorporation of a single molecule of oxygen into a chemical structure as an epoxide or hydroxyl group. These enzymes are predominantly found in the liver and intestines where they are involved in the metabolism of xenobiotics. CYP enzymes that are found in many other extrahepatic tissues, including the kidney, nasal mucosa, and brain, are highly involved in the bioactivation of endogenous products (Zhang et al., 2005; Kalsotra et al., 2006). In several tissues, such as the kidney and brain, the predominant CYP isoforms expressed are involved in endogenous substrate bioactivation (Meyer et al., 2007), rather than xenobiotic metabolism.

One such role for the CYP enzyme system in endogenous substrate bioactivation is the mono-oxygenation of arachidonic acid to form potent vasoactive eicosanoids. Specifically, CYP enzymes catalyze the epoxygenation at the double bonds of arachidonic acid to form epoxyeicosatrienoic acids (EETs) (Luo et al., 1998). CYP enzymes also catalyze the hydroxylation of arachidonic acid on the terminal carbons to form several hydroyeicosatetraenoic acids (HETEs). EET and HETE metabolites produce a growing number of effects on vascular smooth muscle and other tissues. Specifically the terminal hydroxylation of arachidonic acid to form 20-HETE produces potent microvascular vasoconstriction (Harder et al., 1994), mediates angiogenic effects (Amaral et al., 2003), and has been shown to augment vascular smooth muscle cell migration (Stec et al., 2007). Collectively, these studies suggest that the mono-oxygenation pathways of arachidonic acid metabolism are highly potent regulators of microvascular tone and growth.

Growing evidence has implicated 20-HETE in the pathogenesis of cardiovascular and neurovascular disease. Animal studies have demonstrated that inhibition of 20-HETE formation is neuroprotective in temporary focal ischemia and subarachnoid hemorrhage models (Takeuchi et al., 2005; Omura et al., 2006; Poloyac et al., 2006), thereby, implicating 20-HETE as a mediator of ischemic tissue damage. Clinical studies evaluating polymorphisms in the critical enzymes that control 20-HETE production are also supportive of a role for this mono-oxygenated metabolite in diseases of cardiovascular and neurovascular origin (Gainer et al., 2005;; Mayer et al., 2006;). Similarly, prior studies in our laboratory have demonstrated that 20-HETE is also found in human cerebrospinal fluid after subarachnoid hemorrhage (Poloyac et al., 2005).

Due to the multitude of actions of 20-HETE, specific chemical inhibitors are in development to elucidate the role of 20-HETE in disease pathogenesis. The majority of 20-HETE inhibitors have targeted the enzymatic formation by the CYP4A and CYP4F isoforms. These 20-HETE inhibitors include 17-octadecynoic acid (17-ODYA), N-methylsulfonyl-12,12-dibromododec-11-enamide (DDMS), N-Hydroxy-N'-(4-n-butyl-2-methylphenyl)formamidine (HET0016), and, more recently, N-(3-chloro-4-morphlin-4yl-N'hydroxyimidoformamide (TS-011) (Miyata et al., 2005; Omura et al., 2006). Of these inhibitors, the HET0016 and TS-011 compounds share similar structural characteristics and presumably similar mechanisms of CYP enzyme inhibition (Nakamura et al., 2003; Seki et al., 2005). HET0016 is a specific, commercially available inhibitor of 20-HETE. Due to its specificity, potency and availability, HET0016 is being used as an experimental tool to determine the *in vivo* and *in vitro* role of 20-HETE formation in various disease states.

One of the limitations of the use of HET0016 for *in vivo* studies has been the poor aqueous solubility of the compound and the limited knowledge about the time course and mechanism of inhibition. Furthermore, little information exists about the tissue selectivity and the *in vivo* concentration necessary for inhibition of 20-HETE in the rat brain tissues. In order to better understand the pharmacologic utility of HET0016, our laboratory set out to elucidate the effects of HET0016 on the enzymatic formation of 20-HETE in the rat brain. A secondary purpose of this work was to determine the dose/concentration response relationship for 20-HETE inhibition in the rat brain.

MATERIALS AND METHODS

Materials. Arachidonic Acid, 20-HETE, and 20-HETE-d6 metabolites were purchased from Cayman Chemicals (Ann Arbor, MI). N-(4-Butyl -2 - methylphenyl) - N'-hydroxyiminoformamide (HET0016) was purchased from Ryan Scientific (Isle of Palms, SC). Organic solvents were purchased from ThermoFisher Scientific Co. (Pittsburgh, PA) and all other chemicals were purchased from Sigma-Aldrich (St. Louis, MO) unless otherwise specified.

Animals. Male Sprague-Dawley rats (body weight, 250-300g) were obtained from Hilltop Laboratory Animals Inc., (Scottsdale, PA). The animals were maintained on a 12-hour light/dark cycle and were given free access to pellets and water. Rats were placed under light anesthesia with 3:1 ketamine and xylazine (v/v) (Webster Veterinary Supply, Sterling, MA) or performed by the employment of a spontaneous inhalational anesthesic system (SurgiVet V7216 Isotec 4) using isoflurane in conjunction with pure oxygen and nitrous oxide. Animals were sacrificed by decapitation, and brain cortical tissue was excised. A separate set of animals received a bilateral temporary femoral cannulas via insertion of 50 guage polyethylene tubing. A single intravenous (iv) injection of HET0016 1 mg/kg in 15% HPβCD, or vehicle was administered via one of the two femoral cannuals and blood samples were obtained via the opposite femoral cannula for serum isolation. Animals were sacrificed at multiple time-points and brain cortical tissue was harvested. All animal procedures were approved by the Institutional Animal Care and Use Committee of the University of Pittsburgh.

Solubility.

To determine the solubility of HET0016, 0.5mg was added to 1mL of distilled, deionized water (ddH2O) and 0.5mg was added to 1mL of 15% HPβCD (n = 6). Both groups agitated for 48 hours at room temperature on a Titer Plate Shaker (Lab – Line Instruments, Inc., Melrose Park, IL) set at a speed of 450rpm. At the end of the agitation period, both groups were lyophilized to complete dryness using a Freezone 6 Lyopholizer (Labcono Inc., Kansas City, MO), reconstituted in 1mL of ddH2O and syringe-filtered using Millipore® 0.45µm, 13mm polyvinylidene difluoride (PVDF) Syringe Filters (Fisher Scientific, Pittsburgh, PA). HET0016 HPβCD solubility was determined by adding varying amounts of HET0016 to 1mL of 15% HPβCD. The amounts of HET0016 used were 0.5mg, 0.75mg, 1mg, 1.25mg, 1.5mg, 1.75mg and 2 mg (n = 3). After the addition of HET0016, samples were isolated and lyophilized for subsequent HET0016 concentration determination.

Formulation.

Formulation of HET0016 with HPβCD was achieved by adding 0.5mg of HET0016 to 1mL of 15% HPβCD and agitating at room temperature for 48 hours on a Titer Plate Shaker (Lab – Line Instruments, Inc., Melrose Park, IL) set at a speed of 450 rpm. At the end of the agitation period, the samples were lyophilized to complete dryness with a Freezone 6 Lyopholizer (Labcono Inc., Kansas City, MO). Samples were reconstituted with phosphate-buffered saline (PBS) and syringe filtered using Millipore® 0.45µm, 133mm PVDF Syringe Filters (Fisher Scientific, Pittsburgh, PA) before administering to animals.

Microsomal Preparation. Brain cortical tissue was homogenized in cold buffer (50mM tris buffer, 150mM KCl, 0.1 mM dithiothreitol, 1 mM EDTA, and 20% glycerol, pH 7.4) containing 0.1 mM PMSF and 0.113 mM BHT. Microsomes were obtained via differential centrifugation in a Beckman Coulter Optima XL-100K ultracentrifuge (Beckman Coulter, Fullerton, CA) as previously described by Rockich and Blouin (1999). Total microsomal protein was determined by the method detailed by Lowry et al. (1951).

Cortical Microsome Inhibition Study. Brain cortical microsomes from untreated animals were incubated with HET0016 (48.5nM) with and without a 10 minute pre-incubation step to determine the mechanism of inhibition. Incubations, containing 320µg of microsomal protein, consisted of 100µM of arachidonic acid in a 1 ml volume of incubation buffer (0.12 M potassium phosphate buffer containing 5mM magnesium chloride). Reactions were initiated by the addition of 1mM NADPH with a subsequent 1mM concentration added 30 minutes afterwards. Incubations were carried out at 37ºC for 60 minutes and the reaction was stopped by placing the tubes on ice. To each sample, 75 ng of 20-HETE d6 was added as the internal standard. Microsomal incubations were extracted twice with three milliliters of diethyl ether, dried under nitrogen gas, and reconstituted in 80:20 methanol: deionized water.

In a subsequent study, brain cortical microsomes from untreated animals were incubated with or without HET0016 (24.2nM) and analyzed for 20-HETE formation under varying substrate concentrations. Incubations, containing 325ug of microsomal protein, were conducted over arachidonic acid concentrations ranging from 0.2-120 µM in a 1 ml volume of incubation buffer and the reaction was carried out as previously described.

Incubations of brain cortical microsomes were prepared from vehicle-treated or HET0016-treated animals (n = 6 per treatment group) were carried out using 325µg of microsomal protein. Tissue was harvested one hour after iv dose administration for subsequent ex vivo assessment of 20-HETE formation. Brain microsomes were incubated in the presence of 100µM arachidonic acidin order to determine the degree of 20-HETE formation.

Tissue Extraction. 20-HETE and HET0016 concentrations were determined in brain cortical tissue samples of vehicle-treated and inhibitor-treated animals using solid phase extraction as previously described by Poloyac et al. (2004) with minor modifications. Briefly, tissue samples were homogenized in a 0.12 M potassium phosphate buffer containing 5mM magnesium chloride and 0.113mM BHT and centrifuged for 30 minutes at 10,000rpm. The supernatant was removed, 7.5 ng of 20-HETE d6, and 6.6ng of N1-(4-butyl-2-methylphenyl) acetamide (Maybridge, Cambridge, UK) were added as the internal standards, and samples were extracted using HLB solid phase extraction cartridges (Oasis, Waters, Milford, MA). Columns were washed with three 1 ml volumes of 5% methanol and were eluted with 100% methanol. Extracts were dried under nitrogen gas at 37ºC and reconstituted in 200ul of 80:20 methanol: deionized water.

HET0016 Validation. Validation of the quantitative assay was performed by using eight standard concentrations of HET0016, prepared in a 1 ml volume of incubation buffer, and extracted via solid phase extraction using the above method. The amounts of HET0016 in the standards ranged from 0.05 to 2 ng injected on column. Duplicate standard curves were prepared

and analyzed over three runs. Curves were calculated based on the peak-area ratios of HET0016 to the internal standard and plotted against the amount of HET0016 injected onto the column. Calibration curves were generated by weighted (1/Y) linear regression. Precision and accuracy were determined by the analysis of HET0016 quality control (QC) samples. HET0016 was spiked into buffer to yield low, medium, and high QCs, corresponding to 0.09, 0.45, and 1.25 ng on column, respectively. Six samples at each level were analyzed for two days, followed by 12 replicates of each on the final day of validation. Accuracy was determined by comparing the concentrations measured in the quality control samples with respect to known values and expressed as relative standard error (% bias). Precision was evaluated by measuring separately prepared QCs and expressed as relative standard deviation of the mean concentrations. Recovery of HET0016 was estimated by comparing the area ratios of extracted samples to those of neat samples prepared in respective concentrations in 80:20 methanol:deionized water.

Chromatographic Conditions. HPLC was performed using a ThermoFinnigan Surveyor Autosampler (ThermoFinnigan, San Jose, CA). Separation of 20-HETE was conducted on a Betabasic C-18, 5µm (150 x 2.1mm) reversed-phase column (ThermoHypersil, Bellefont, PA) under ambient temperature at a flow rate of 0.2ml/min. Mobile phases consisted of 5mM ammonium acetate in deionized water (A) and methanol (B) at an initial mixture of 40:60. Mobile phase B increased from 60% to 98% in a linear gradient over 11 minutes, and remained there over the next two minutes. This was followed by a linear return to initial conditions over 0.2 minutes with a four minute pre-equilibration period prior to the next sample run. Total run time per sample was 17.2 minutes and all injection volumes were 10 µl or 20 µl on column.

Separation of HET0016 was conducted using the above methods, with a slight modification in the gradient. From an initial mixture of 40:60 A:B, mobile phase B increased from 60% to 95% in a linear gradient over 11 minutes, ramped again up to 98% over one minute, and remained there over the next four minutes. This was followed by a linear return to initial conditions over 0.2 minutes with a three minute pre-equilibration period prior to the next sample run. Total run time per sample was 19.2 minutes and all injection volumes were 10 µl and 20 µl on column.

Mass Spectrometric Conditions. Mass spectrometric analysis of 20-HETE formation was performed using a ThermoFinnigan MSQ single quadrupole mass spectrometer and a ThermoFinnigan TSQ Quantum Ultra triple quadrupole mass spectrometer, both operated in negative electrospray ionization (ESI) mode. Analysis was carried out on the MSQ with a probe temperature and voltage of 350º C and 3.0kV, respectively. Cone voltage was set at 75V and selective ion monitoring (SIM) was carried out for specific m/z 320.5 (20-HETE) and m/z 326.5 (20-HETE d6, internal standard). Analysis was carried out on the TSQ operated in negative ESI selected reaction monitoring (SRM) mode with unit resolutions at both Q1 and Q3 set at 0.70 full width at half maximum (FWHM). The SRM transitions of m/z 319.3 → 245 (collision energy 15eV, scan time 0.20 s) for 20-HETE and m/z 325.3 → 251 (collision energy 15eV, scan time 0.20 s) for IS were monitored. Parameters were optimized to obtain the highest [M-H]+ ion abundance and were as follows: capillary temperature 350º C, spray voltage 3500 kV, and source collision-induced dissociation (CID) set at 0V. Sheath gas, auxiliary gas, and ion sweep gas pressures were set at 50, 20, and 0, respectively. Collision gas pressure was set at 1.2 mTorr. Mass spectrometric analysis of HET0016 was performed using a ThermoFinnigan MSQ single quadrupole mass spectrometer and a ThermoFinnigan TSQ Quantum Ultra triple quadrupole

mass spectrometer, both operated in positive electrospray ionization (ESI) mode. Analysis was carried out on the MSQ (supplemented with a cone wash using 100% MeOH), with a probe temperature of 350ºC and a needle voltage of 3.8kV. Cone voltage was set at 63V and selective ion monitoring (SIM) was carried out for specific m/z 207.15 (HET0016) and m/z 206.29 (IS). Detection of HET0016 in brain cortical tissue extracts was employed using the TSQ Quantum Ultra system operated in positive ESI selected reaction monitoring (SRM) mode with unit resolutions at both Q1 and Q3 set at 0.70 full width at half maximum (FWHM). The SRM transitions of m/z 207 → 130 (collision energy 31eV, scan time 0.10 s) for HET0016 and m/z 206 → 108.1 (collision energy 21eV, scan time 0.10 s) for IS were monitored. Capillary temperature was set at 350ºC, spray voltage was set at 4200 kV, and source collision-induced dissociation (CID) was set at 0V. Sheath gas, auxiliary gas, and ion sweep gas pressures were set at 50, 20, and 5, respectively. Collision gas pressure was set at 1.2 mTorr. Analytical data was acquired and analyzed using Xcaliber software version 1.4 (ThermoFinnigan, San Jose, CA).

Pharmacokinetic Parameter Determination and Statistical Methods.

HET0016 pharmacokinetic parameters estimates were determined by non-compartmental methods using WinNonlin version 4.1. An unpaired student's t- test was performed for comparisons between two groups, whereas, a one-way analysis of variance (ANOVA) was performed for comparisons between three or more group comparisons with individual differences determined via a Dunnett's multiple comparison post-hoc. Values that are statistically significant are designated by asterisks (*) $p < 0.05$ and (**) $p < 0.01$. Statistical analyses were performed using PRISM Graph Pad version 2004.

RESULTS

Quantitative Measurement of HET0016 by HPLC MS/MS

The utility of a solid phase extraction HPLC MS/MS as a quantitative method for reproducibly determining HET0016 concentrations was evaluated. A solid phase extraction method that allowed for simultaneous extraction of HET0016 and 20-HETE was developed. Figure 1 depicts the subsequent HPLC MS/MS chromatograph for HET0016 and 20-HETE along with their respective internal standards. Table 1 presents the intraday and interday variability of the solid phase extraction HPLC MS/MS method. All coefficients of variation were less than 10% over a range of 50 to 2000 pg on column.

Mechanism of HET0016 Inhibition of 20-HETE Formation

Formation of 20-HETE in incubations containing rat brain cortical microsomes (325 μg total protein), NADPH (1 μM), and arachidonic acid (0.2 – 70 μM), in the presence and absence of HET0016 (24nM) were determined. As depicted in Figure 2A, maximal 20-HETE formation rate in vehicle control microsomes was 10.2 pmol/mg/min with saturation observed at arachidonic acid concentrations above 30 μM. Co-incubation with 24 nM HET0016 reduced the maximal formation rate to 0.69 pmol/mg/min. Inhibition of 20-HETE formation in rat brain cortical microsomes persisted despite increasing concentrations of arachidonic acid. Concentrations up to 120 μM arachidonic acid incubated in the presence of 24 nM HET0016 did not alter the formation rate, thereby, demonstrating non-competitive inhibition by HET00016.

In order to determine if HET0016 required metabolic conversion to an active inhibitory metabolite, we evaluated the inhibitory activity of HET0016 with and without preincubation prior to arachidonic acid addition. As depicted in Figure 2B, HET0016 inhibited 20-HETE formation under both pre-incubation and without pre-incubation conditions with no significant difference in formation between these two groups. Formation rates in pre-incubation and without preincubation were 4.92 ± 0.19 % and 4.89 ± 0.46 % of control incubation formation rates, respectively.

HET0016 Inhibition of 20-HETE Formation

Brain cortical microsomes were incubated with arachidonic acid in the presence or absence of HET0016 to determine the inhibition of 20-HETE formation in microsomes. Figure 3A demonstrates that rat brain cortical microsomal formation rate wasinhibited by HET0016 with significant inhibition at 30 nM (1.81 ±1.14 pmol/mg/min) and 90 nM (0.92 ± 0.02 pmol/mg/min) concentrations as compared to control (6.46 ± 2.5 pmol/mg/min). In addition, rats were treated in vivo with 1 mg/kg HET0016 or lecithin vehicle followed by sacrifice and tissue harvesting 1 hour after dosing. Brain cortical microsomes were harvested for ex vivo evaluation of 20-HETE microsomal formation in the absence of inhibitor. Figure 3B demonstrates the 20-HETE formation rate in microsomes obtained from treated and untreated animals.

Solubility and In Vivo Kinetics of an HET0016 / Hydroxypropyl-beta-cyclodextrin (HPβCD) Formulation

The effect of HPβCD on the aqueous solubility of HET0016 was evaluated as a potential method to increase the aqueous solubility of HET0016 for intravenous administration. Figure 4

demonstrates the increase in aqueous solubility of HET0016 in a formulation containing 15% HPβCD as compared to the intrinsic solubility in ddH_2O after 48 hours of incubation. Aqueous solubility of HET0016 was increased from 34.2 μg/mL in ddH_2O to 452.7μg/mL in 15% HPβCD.

The HPβCD formulation of HET0016 (1 mg/kg) was administered intravenously with serial plasma sampling at 0, 5, 10, 30, 60, 80, 120, 150, and 180 minutes after dose administration (n=4). Figure 5 depicts the log plasma concentration versus time curve after iv bolus administration of cyclodextrin complexed HET0016. This plasma concentration versus time profile suggests rapid elimination of HET0016. Non-compartmental pharmacokinetic estimates of clearance, volume of distribution, and half-life are reported in Table 2.

Brain 20-HETE Formation after Intravenous Administration of HET0016

A total of forty rats were serially sacrificed for measurement of 20-HETE concentration in cortical brain tissue at 0, 5, 10, 30, 60, 180, 360 and 1440 minutes after HET0016 single iv dose administration (n=5 per time point). As depicted in Figure 6, tissue concentrations of 20-HETE were decreased within five minutes of dose administration and remained significantly reduced for 60 minutes. Consequently, the 20-HETE concentration partially recovered to 70% at 180 minutes and returned to control levels by 24 hours. In addition, the brain to plasma ratio of HET0016 was also determined at the 5, 10, 30, and 60 minute time points after HET0016 administration. The HET0016 brain cortical tissue to plasma ratio was 7.5 ± 1.1 at 5 minutes, 9.5 ± 1.6 at 10 minutes, 2.9 ± 0.5 at 30 minutes, and 2.2 ± 0.3 at 60 minutes. The time course of cortical tissue and plasma concentrations in these animals is presented in Figure 7.

DISCUSSION

The results of this manuscript demonstrate the following significant findings: 1) HET0016 is a non-competitive inhibitor of 20-HETE formation that does not require metabolic activation in rat brain microsomes 2) Formulation of HET0016 with HPβCD yields over a 10-fold increase in the aqueous solubility of HET0016, allowing for intravenous administration 3) HET0016 is highly distributed into the brain and rapidly inhibits 20-HETE formation in brain tissue after intravenous administration of the HET0016/HPβCD formulation. To our knowledge, our data are the first to determine the tissue kinetics of altered 20-HETE concentrations following administration of HET0016. Furthermore, the results of this study are significant in that they demonstrate that a formulation of HET0016/HPβCD is an effective method to elucidate the dose-inhibition response relationship of 20-HETE inhibition in the rat brain.

Our conclusion that HET0016 is a selective, non-competitive inhibitor of 20-HETE formation in rat brain microsomes is based on the observation that HET0016 (24 nM) reduced the maximum velocity of 20-HETE formation *in vitro* that was unaltered by increasing arachidonic acid concentrations. These data are consistent with a previous report by Seki et al. (2005) who demonstrated that HET0016 at concentrations of 20 and 40 nM reduced Vmax without altering Km in cell membranes from a recombinant CYP4A1 expression system, thereby, implying non-competitive inhibition. In study by Miyata et al. (2001), EET metabolites were combined to determine the effect of the inhibitor on 20-HETE versus the sum total of EET peaks observed in the kidney microsomal systems. This study demonstrated that HET0016 has a selectivity window for 20-HETE inhibition at 10^{-6} to 10^{-7} M concentrations, whereas, the mechanism of HET0016 inhibition in kidney microsomes was not determined in this study. These results are

also consistent with previous studies by our laboratory that have demonstrated that HET0016 specifically inhibits microsomal formation of 20-HETE as compared to individual EETs (Poloyac et al., 2006).

Prior studies have suggested that although HET0016 is highly distributed and is a very potent inhibitor of 20-HETE formation, its use is limited by its poor aqueous solubility at neutral pH and the instability of HET0016 at acidic pH (Nakamura et al., 2003). This led to studies exploring new pyrazole and isoxazole derivatives of HET0016 as new chemical inhibitors of this pathway. In the present study, we demonstrated that a hydroxypropyl-β-cyclodextrin formulation of HET0016 greatly increases the aqueous solubility of this compound and thereby creates a useful intraveneous form. Furthermore, we demonstrated that this formulation of HET0016 produces a reproducible plasma profile and exhibited rapid brain disposition and reductions in 20 HETE within 5 minutes of administration. This observation is consistent with multiple other studies that have successfully employed HPβCD to increase the aqueous solubility of small molecules for intravenous administration (Jarho et al., 1995; Trapani et al., 1998; Govindarajan and Nagarsenker, 2005). Furthermore, the concentrations of 15% HPβCD administered as a 1 ml solution intravenously have been employed previously without adverse effects in animal models and humans (Pitha et al., 1988; Gould and Scott, 2005). Collectively, these data suggest that a formulation of HET0016 with HPβCD is a viable method for *in vivo* inhibition of 20-HETE in the rat brain, thereby facilitating future studies to determine the role of 20-HETE in the pathogenesis of neurovascular disease.

Solid phase extraction with HPLC MS/MS detection of HET0016 was demonstrated as a reproducible method for the quantification of tissue concentrations. This extraction method is the same method previously reported by our laboratory for the quantification of 20-HETE (Poloyac et al., 2005). Although these methods differ in mass spectrometric detection conditions, quantification of 20-HETE and HET0016 can be completed via sequential injections of a single tissue extract by this method.

The pharmacokinetic parameter estimates demonstrate that HET0016 has a short biological half-life. Previously, our laboratory determined pharmacokinetic parameter estimates after intraperitoneal administration of a 10 mg/kg dose of HET0016 dissolved in lecithin (Poloyac et al., 2006). Brain concentrations were less than 10% of plasma concentrations at 1 hour after intraperitoneal dosing in our previous study as compared to 220% at 1 hour after HET0016/HPβCD intravenous dosing in the present study. Although this is not a direct comparison of dosage routes and formulations, we can state that lower doses of intravenous HET0016/HPβCD are required for brain inhibition of 20-HETE potentially due to greater brain penetration; however, continuous infusion is likely to be necessary to maintain this inhibition in the brain due to the short biological half-life of HET0016 *in vivo*.

In summary, the results of this study provide evidence that HET0016 is a non-competitive inhibitor of brain cortical 20-HETE formation. We also demonstrate that despite its low intrinsic aqueous solubility, HET0016 can be formulated with HPβCD to increase aqueous solubility for intravenous administration. Furthermore, we demonstrated that HET0016 produces a very rapid, short duration inhibition of 20-HETE formation after single dose administration. These data will

allow for future studies to elucidate the *in vivo* pharmacology and mechanism of inhibition by HET0016 and the role of 20-HETE in diseases of neurovascular origin.

REFERENCES

Amaral SL, Maier KG, Schippers DN, Roman RJ and Greene AS (2003) CYP4A metabolites of arachidonic acid and VEGF are mediators of skeletal muscle angiogenesis. *Am J Physiol Heart Circ Physiol* **284:**H1528-H1535.

Gainer JV, Bellamine A, Dawson EP, Womble KE, Grant SW, Wang Y, Cupples LA, Guo CY, Demissie S, O'Donnell CJ, Brown NJ, Waterman MR and Capdevila JH (2005) Functional variant of CYP4A11 20-hydroxyeicosatetraenoic acid synthase is associated with essential hypertension. *Circulation* **111:**63-69.

Gould S and Scott RC (2005) 2-Hydroxypropyl-beta-cyclodextrin (HP-beta-CD): a toxicology review. *Food Chem Toxicol* **43:**1451-1459.

Govindarajan R and Nagarsenker MS (2005) Formulation studies and in vivo evaluation of a flurbiprofen-hydroxypropyl beta-cyclodextrin system. *Pharm Dev Technol* **10:**105-114.

Harder DR, Gebremedhin D, Narayanan J, Jefcoat C, Falck JR, Campbell WB and Roman RJ (1994) Formation and action of a P-450 4A metabolite of arachidonic acid in cat cerebral microvessels. *Am J Physiol* **266:**H2098-H2107.

Jarho P, Urtti A and Jarvinen T (1995) Hydroxypropyl-beta-cyclodextrin increases the aqueous solubility and stability of pilocarpine prodrugs. *Pharm Res* **12:**1371-1375.

Kalsotra A, Zhao J, Anakk S, Dash PK and Strobel HW (2006) Brain trauma leads to enhanced lung inflammation and injury: evidence for role of P4504Fs in resolution. *J Cereb Blood Flow Metab*.

Luo G, Zeldin DC, Blaisdell JA, Hodgson E and Goldstein JA (1998) Cloning and expression of murine CYP2Cs and their ability to metabolize arachidonic acid. *Arch.Biochem.Biophys.* **357:**45-57.

Mayer B, Lieb W, Gotz A, Konig IR, Kauschen LF, Linsel-Nitschke P, Pomarino A, Holmer S, Hengstenberg C, Doering A, Loewel H, Hense HW, Ziegler A, Erdmann J and Schunkert H (2006) Association of a functional polymorphism in the CYP4A11 gene with systolic blood pressure in survivors of myocardial infarction. *J Hypertens* **24:**1965-1970.

Meyer RP, Gehlhaus M, Knoth R and Volk B (2007) Expression and Function of Cytochrome P450 in Brain Drug Metabolism. *Curr Drug Metab* **8:**297-306.

Miyata N, Seki T, Tanaka Y, Omura T, Taniguchi K, Doi M, Bandou K, Kametani S, Sato M, Okuyama S, Cambj-Sapunar L, Harder DR and Roman RJ (2005) Beneficial effects of a new 20-hydroxyeicosatetraenoic acid synthesis inhibitor, TS-011 [N-(3-chloro-4-morpholin-4-yl) phenyl-N'-hydroxyimido formamide], on hemorrhagic and ischemic stroke. *J Pharmacol Exp Ther* **314:**77-85.

Miyata N, Taniguchi K, Seki T, Ishimoto T, Sato-Watanabe M, Yasuda Y, Doi M, Kametani S, Tomishima Y, Ueki T, Sato M and Kameo K (2001) HET0016, a potent and selective inhibitor of 20-HETE synthesizing enzyme. *Br.J Pharmacol.* **133:**325-329.

Nakamura T, Sato M, Kakinuma H, Miyata N, Taniguchi K, Bando K, Koda A and Kameo K (2003) Pyrazole and isoxazole derivatives as new, potent, and selective 20-hydroxy-5,8,11,14-eicosatetraenoic acid synthase inhibitors. *J Med Chem* **46:**5416-5427.

Omura T, Tanaka Y, Miyata N, Koizumi C, Sakurai T, Fukasawa M, Hachiuma K, Minagawa T, Susumu T, Yoshida S, Nakaike S, Okuyama S, Harder DR and Roman RJ (2006) Effect of a new inhibitor of the synthesis of 20-HETE on cerebral ischemia reperfusion injury. *Stroke* **37:**1307-1313.

Pitha J, Irie T, Sklar PB and Nye JS (1988) Drug solubilizers to aid pharmacologists: amorphous cyclodextrin derivatives. *Life Sci* **43:**493-502.

Poloyac SM, Reynolds RB, Yonas H and Kerr ME (2005) Identification and quantification of the hydroxyeicosatetraenoic acids, 20-HETE and 12-HETE, in the cerebrospinal fluid after subarachnoid hemorrhage. *J Neurosci Methods* **144:**257-263.

Poloyac SM, Zhang Y, Bies RR, Kochanek PM and Graham SH (2006) Protective effect of the 20-HETE inhibitor HET0016 on brain damage after temporary focal ischemia. *J Cereb Blood Flow Metab*.

Seki T, Wang MH, Miyata N and Laniado-Schwartzman M (2005) Cytochrome P450 4A Isoform Inhibitory Profile of N-Hydroxy-N'-(4-butyl-2-methylphenyl)-formamidine (HET0016), a Selective Inhibitor of 20-HETE Synthesis. *Biol Pharm Bull* **28:**1651-1654.

Stec DE, Gannon KP, Beaird JS and Drummond HA (2007) 20-Hydroxyeicosatetraenoic acid (20-HETE) stimulates migration of vascular smooth muscle cells. *Cell Physiol Biochem* **19:**121-128.

Takeuchi K, Renic M, Bohman QC, Harder DR, Miyata N and Roman RJ (2005) Reversal of Delayed Vasospasm by an Inhibitor of the Synthesis of 20-HETE. *Am J Physiol Heart Circ Physiol*.

Trapani G, Latrofa A, Franco M, Lopedota A, Sanna E and Liso G (1998) Inclusion complexation of propofol with 2-hydroxypropyl-beta-cyclodextrin. Physicochemical, nuclear magnetic resonance spectroscopic studies, and anesthetic properties in rat. trapani@ippo.uniba.it. *J Pharm Sci* **87:**514-518.

Zhang X, Zhang QY, Liu D, Su T, Weng Y, Ling G, Chen Y, Gu J, Schilling B and Ding X (2005) Expression of cytochrome p450 and other biotransformation genes in fetal and adult human nasal mucosa. *Drug Metab Dispos* **33:**1423-1428.

FOOTNOTES: Authors (YM and MMK) equally contributed to this work. We would like to acknowledge National Institutes of Health NINDS R01NS052315 (SMP) and NCRR S10RR023461 (SMP) for support of this work. We would also like to acknowledge the Pharsight Academic License granted for use in the pharmacokinetic analyses. Corresponding Author: Samuel M. Poloyac, Pharm.D., Ph.D., Associate Professor, 807 Salk Hall, School of Pharmacy, University of Pittsburgh, Pittsburgh, PA 15261, Phone: 412-624-4595, Fax: 412-383-7436, E-mail: poloyac@pitt.edu.

FIGURE 1: High pressure liquid chromatography with triple quadrupole mass spectrometry selective reaction monitoring for detection of 20-HETE and HET0016. Chromatograms from brain tissue extracts analyzed for 20-HETE (319 → 245), d6-20-HETE (325 → 251), HET0016 (207 → 130***), and N1-(4-butyl-2-methylphenyl) acetamide (206 → 108) are presented in Panels A through D, respectively. Brain cortical tissue was harvested from vehicle control (Panels A and B) and HET0016 (Panels C and D) treated animals. Tissues from individual animals underwent a single solid phase extraction followed by MS/MS analysis for 20-HETE and HET0016 as described in the Materials and Methods section. The developed extraction method allows for the subsequent analysis of both 20-HETE and HET0016 from the same tissue samples. 20-HETE concentrations in HET0016 treated animals were near or below the limits of detection (data not shown).

FIGURE 2: Elucidation of the mechanism of HET0016 mediated inhibition of 20-HETE formation. Panel A depicts the effect of HET0016 on the *in vitro* formation of 20-HETE by rat brain cortical microsomes. Incubations contained 325 μg rat brain cortical microsomal total protein, 1 μM NADPH, arachidonic acid 0.2 – 70 μM, in the presence and absence of 24nM HET0016. These data demonstrate that HET0016 is a non-competitive inhibitor of 20-HETE formation in rat brain cortical microsomes. Panel B depicts the effect of preincubation of microsomes with HET0016 prior to the addition of arachidonic acid on the formation rate of 20-HETE in rat brain cortical microsomes. These data demonstrate that HET0016 does not require metabolic activation in order to inhibit 20-HETE formation, therefore, is not acting as a suicide substrate or mechanistic inhibitor of 20-HETE formation. Statistically significant differences are denoted by an asterisk (*) $p < 0.01$.

FIGURE 3: Effect of HET0016 on 20-HETE formation after *in vitro and ex vivo incubation* . Panel A: control rat brain cortical microsomes were isolated and incubated in the presence of HET0016 30nM, HET0016 90nM, or vehicle control (n = 6 per data point). These data demonstrate that HET0016 at the 30nM concentration produced a ~70% reduction in 20-HETE formation rate Panel B: Rats were treated with HET0016 (1 mg/kg) or lecithin control intravenously and were sacrificed one hour later for measurement of 20-HETE formation in microsomes ex vivo. Microsomes were isolated from HET0016 and vehicle treated animals one hour after dosing. In vitro 20-HETE formation was then assessed in the absence of inhibitor. This figure depicts the persistent inhibition of 20-HETE formation in animals treated with HET0016. Statistically significant differences are denoted by asterisks (*) $p < 0.05$; (**) $p < 0.01$.

FIGURE 4: Formulation of a water soluble hydroxypropyl-β-cyclodextrin conjugate of HET0016. Previously described *in vitro* studies demonstrated the concentrations of HET0016 required for 20-HETE inhibition in the rat brain were 30 to 90nM. In order to target these concentrations *in vivo* a water soluble conjugate of HET0016 forivadministration was required. Complexation reactions were conducted with 15% hydroxypropyl-β-cyclodextrin and varying amounts of HET0016 for 48 hours (Panel A). Aqueous solubility was increased from 34.2 ± 31.2 μg/mL in ddH_2O to 452.7 ± 63.3 μg/mL in 15% hydroxypropyl-β-cyclodextrin (Panel B).

FIGURE 5: Plasma profile of HET0016 after intravenous administration of HET0016 / hydroxypropyl- β-cyclodextrin complex. Depicted in this figure is the plasma concentration versus time profile of HET0016 after intravenous administration of 1 mg/kg of the HET0016 / hydroxypropyl-β-cyclodextrin complex *in vivo* in the rat. After administration of the complex,

HET0016 concentrations were higher than in previous studies that utilized an intraperitoneally or intravenous administration of a lecithin suspension of HET0016 at a dose of 10 mg/kg as published in Poloyac SM et al. J Cerebr Blood Flow Metab 2006; 26(12): 1551-61. Each data point represents the average value ± standard deviation of plasma HET0016 concentrations (n=4).

FIGURE 6: Brain cortical 20-HETE tissue concentrations after intravenous administration of HET0016 / hydroxypropyl- β-cyclodextrin complex. Rats were treated with 1 mg/kg of HET0016 / hydroxypropyl- β-cyclodextrin or hydroxypropyl β-cyclodextrin vehicle control. Rats were sacrificed at various time points after dose administration. Rat brain cortical sections were dissected and evaluated for tissue 20-HETE concentrations. These data demonstrate that a maximal reduction in 20-HETE cortical tissue content of 31.6 ± 4.3% was observed at the 5 minute time point in the HET0016 complex animals as compared to vehicle control. These data demonstrate that the HET0016 / hydroxypropyl-β-cyclodextrin complex is an effective formulation for *in vivo* inhibition of rat brain cortical 20-HETE inhibition by intravenous administration. Each data point is presented as mean ± standard deviation of three to five animals per time point. Statistically significant differences were observed at the 5, 10, 30, 60, 240 ($p < 0.01$) and 120 minute ($p < 0.01$) time points.

FIGURE 7: HET0016 concentrations in brain and plasma after iv bolus administration

Brain tissue and plasma samples were harvested from four to five animals per time point after iv bolus administration of HET0016 (1 mg/kg). The concentration of HET0016 in brain tissue and plasma were determined by LC-MS/MS after solid phase extraction. The brain tissue to plasma concentration ratios of HET0016 were 7.8 ± 1.1 at 5 minutes, 9.5 ± 1.6 at 10 minutes, 2.9 ± 0.5

at 30 minutes, and 2.2 ± 0.3 at 60 minutes, thereby demonstrating rapid distribution into rat brain cortical tissue after iv dosing.

DMD Fast Forward. Published on August 25, 2008 as DOI: 10.1124/dmd.108.023150
This article has not been copyedited and formatted. The final version may differ from this version.

TABLE 1: HET0016 Intra- and Inter-day Precision and Accuracy

	Amount (pg on column)			
	Added	Observed (Mean ± S.D.)	%R.S.D.	% Bias
Intra-assay Reproducibility				
Quality Controls	90	98.5 ± 5.0	5.09	9.46
	450	470.1 ± 30.3	6.44	4.48
	1250	1341 ± 75	5.57	7.25
Inter-assay Reproducibility				
Quality Controls	90	93.3 ± 6.1	6.52	3.68
	450	457.8 ± 18.2	3.97	1.72
	1250	1281 ± 49	3.80	2.51
Standard Curve				
	50	51.9 ± 3.1	5.89	3.75
	75	77.8 ± 8.1	10.36	3.72
	100	96.5 ± 10.1	10.44	-3.47
	250	266 ± 13.6	5.11	6.33
	500	472.9 ± 33.7	7.14	-5.43
	750	745.8 ± 61.8	8.28	-0.56
	1000	979.2 ± 61.6	6.29	-2.08
	2000	2055 ± 83	4.03	2.73

Table 2: HET0016 / HPβCD Non-Compartmental Pharmacokinetic Parameter Estimates

	Average	Standard Deviation
AUC 0 to ∞ [(μg*min)/ml]	20.5	4.9
Clearance[ml/min/kg]	57.4	14.8
Vss [L/kg]	2.4	0.26
t1/2 [min]	39.6	20.0

DMD Fast Forward. Published on August 25, 2008 as DOI: 10.1124/dmd.108.023150
This article has not been copyedited and formatted. The final version may differ from this version.

Figure 1

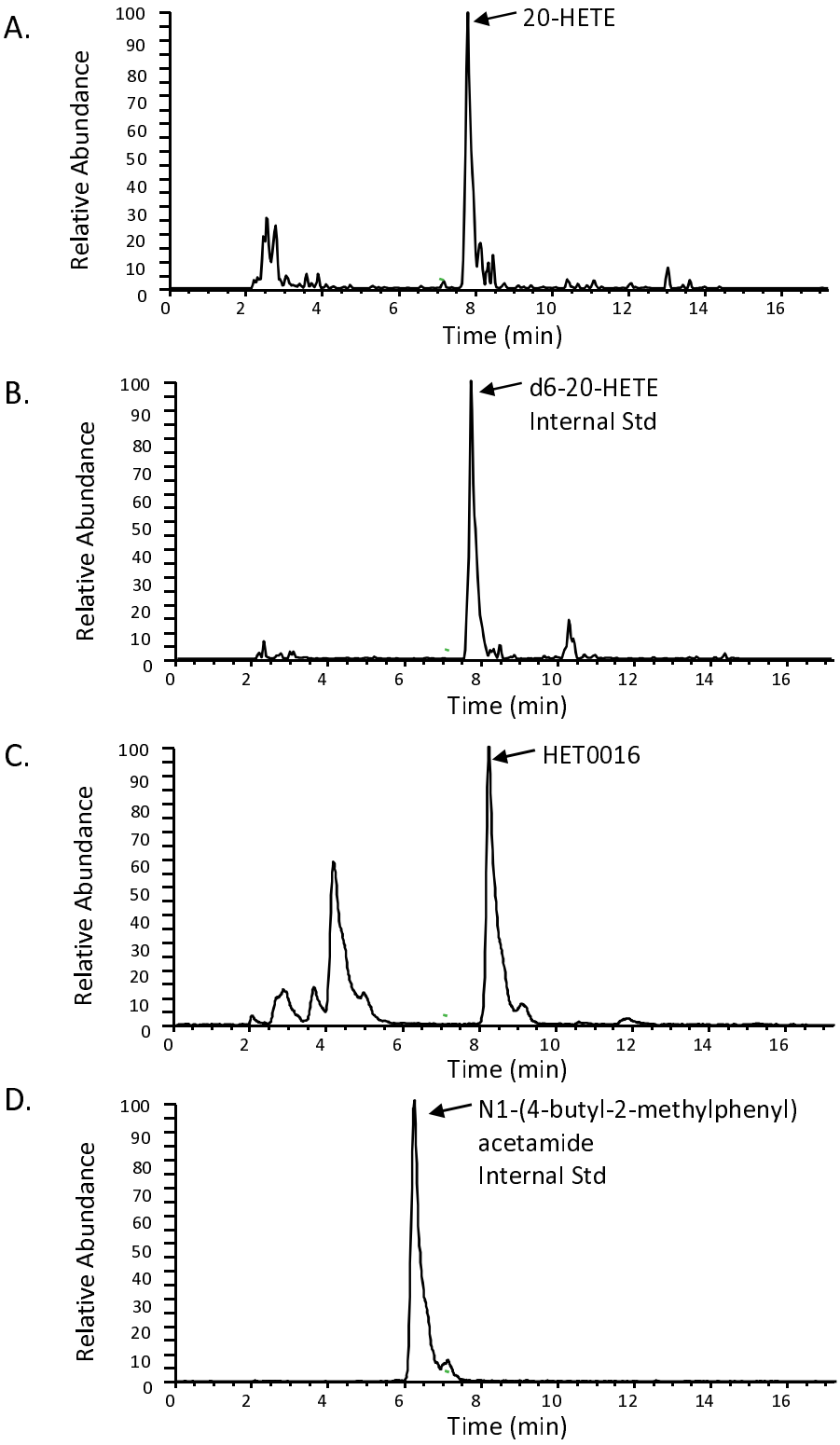

DMD Fast Forward. Published on August 25, 2008 as DOI: 10.1124/dmd.108.023150
This article has not been copyedited and formatted. The final version may differ from this version.

Figure 2

A.

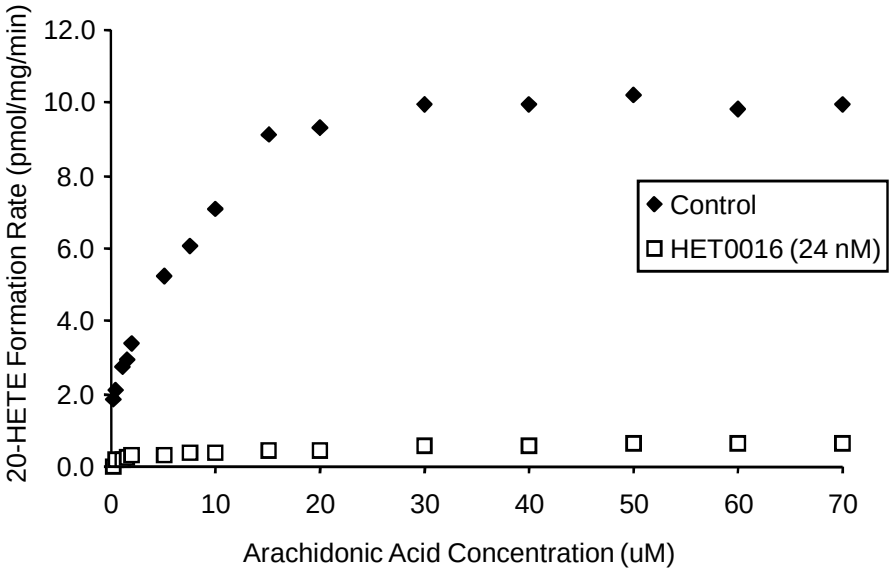

B.

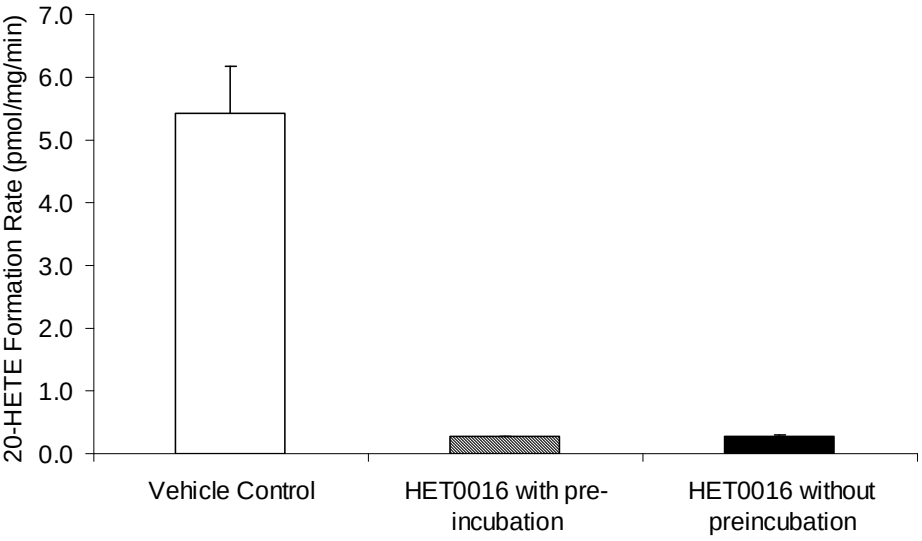

DMD Fast Forward. Published on August 25, 2008 as DOI: 10.1124/dmd.108.023150
This article has not been copyedited and formatted. The final version may differ from this version.

Figure 3

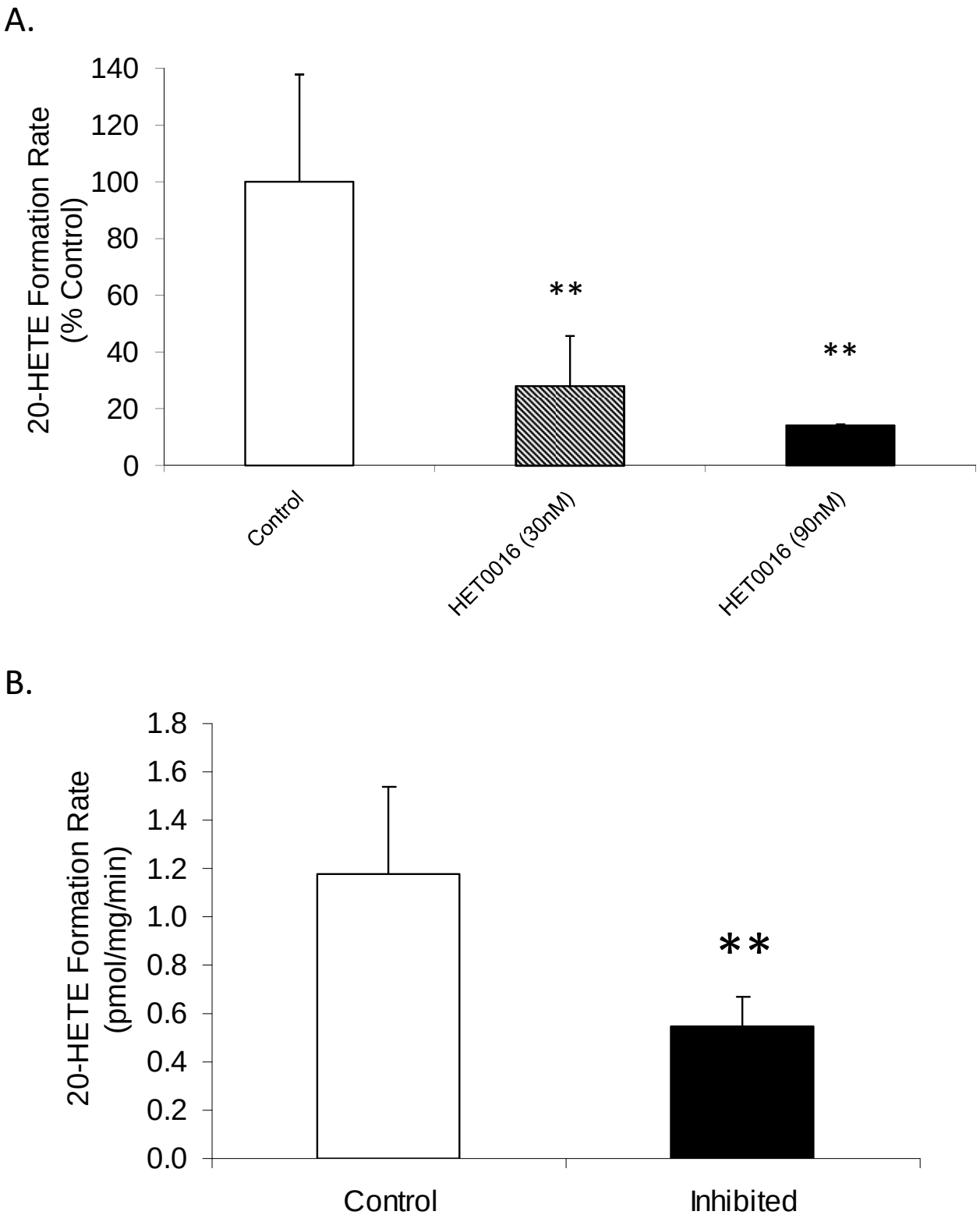

DMD Fast Forward. Published on August 25, 2008 as DOI: 10.1124/dmd.108.023150
This article has not been copyedited and formatted. The final version may differ from this version.

Figure 4

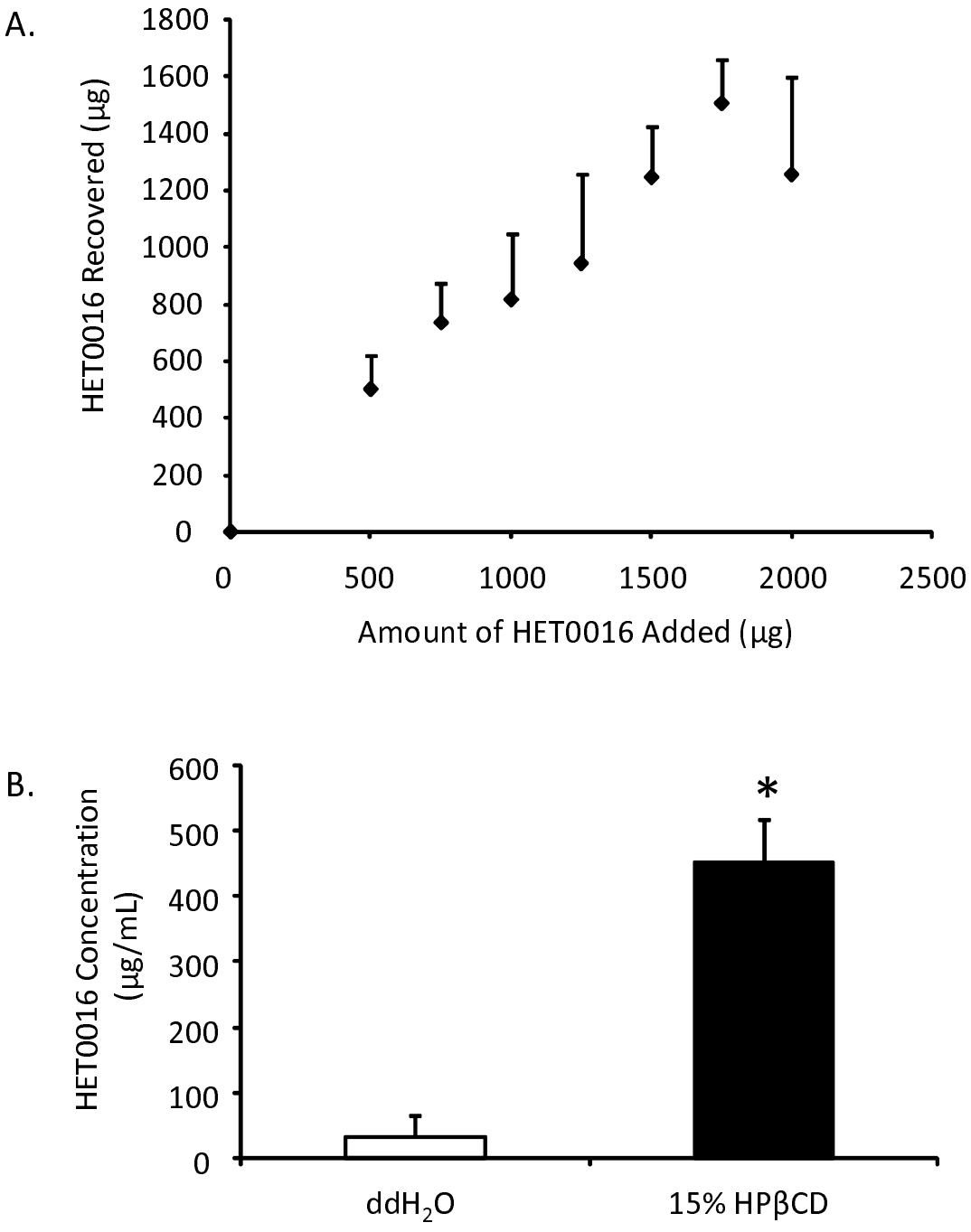

DMD Fast Forward. Published on August 25, 2008 as DOI: 10.1124/dmd.108.023150
This article has not been copyedited and formatted. The final version may differ from this version.

Figure 5

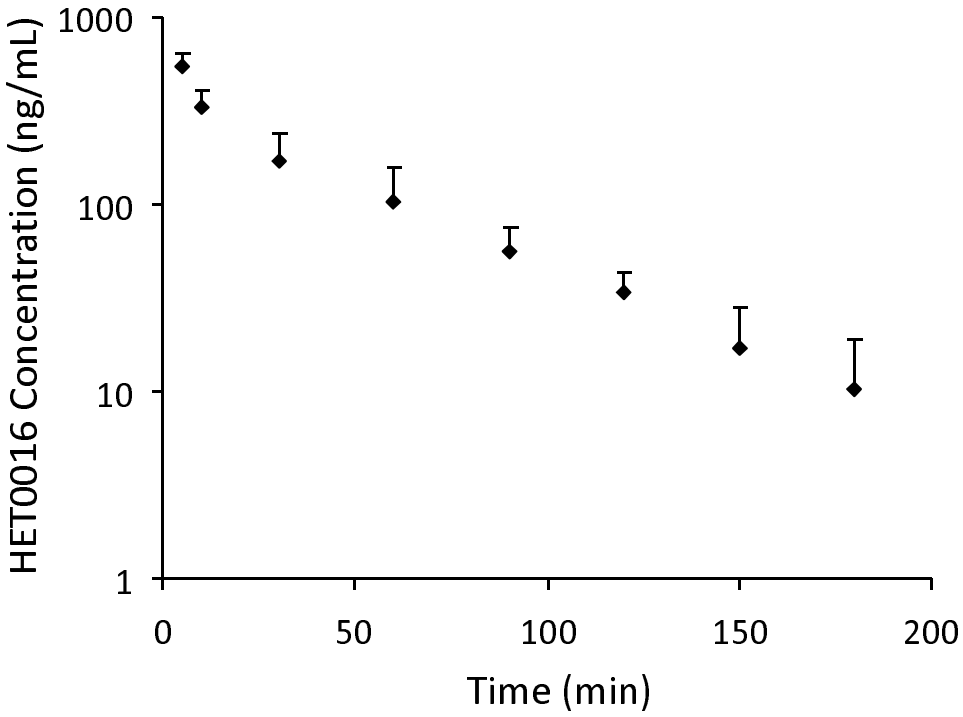

DMD Fast Forward. Published on August 25, 2008 as DOI: 10.1124/dmd.108.023150
This article has not been copyedited and formatted. The final version may differ from this version.

Figure 6

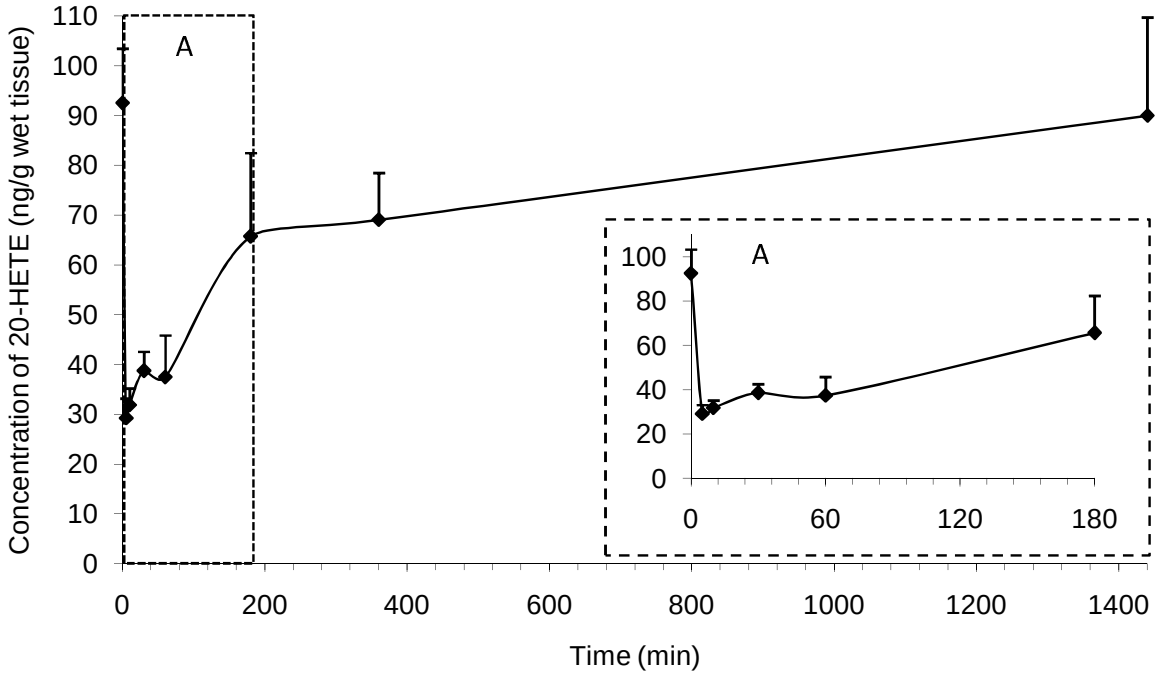

DMD Fast Forward. Published on August 25, 2008 as DOI: 10.1124/dmd.108.023150
This article has not been copyedited and formatted. The final version may differ from this version.

Figure 7